Micromagnetic structures and microscopic magnetization-reversal processes in epitaxial Fe/GaAs(001) elements

E. Gu, E. Ahmad, J. A. C. Bland, and L. M. Brown
Cavendish Laboratory, University of Cambridge, Madingley Road, Cambridge CB3 0HE, United Kingdom

M. Rührig, A. J. McGibbon, and J. N. Chapman
Department of Physics and Astronomy, University of Glasgow, Glasgow G12 8QQ, United Kingdom
(Received 23 June 1997; revised manuscript received 20 November 1997)

The in-plane size and orientation-dependent micromagnetic structures of thin epitaxial Fe(001) elements were studied by Lorentz electron microscopy. It is found that the single-domain remanent state supported by continuous epitaxial films with in-plane anisotropy decays into a multidomain configuration upon reducing the film lateral dimensions. For 150-Å-thick Fe(001) elements, such drastic changes in the remanent domain structure and reversal processes occur when the element size is reduced to $\sim 10\ \mu$m. This transition can be explained as a consequence of the in-plane dipolar (shape anisotropy) contribution to the total energy becoming comparable with that of the magnetocrystalline anisotropy at this size. Due to the interplay between in-plane shape and magnetocrystalline anisotropies, novel micromagnetic phenomena were observed. Distinct microscopic reversal processes arise according to not only the crystallographic direction along which the field is applied but also the orientation of the element edges. For magnetization reversal along the in-plane $\langle 100 \rangle$ directions (easy axes), domains nucleate at either element edges or corners depending on the orientation of element edges. For applied fields aligned along the in-plane $\langle 110 \rangle$ directions (hard axes), a fine-scale stripe (width $\leqslant 200$ nm) domain structure develops upon reducing the applied field from saturation. In addition to coherent rotation and domain-wall displacement, a 90° coherent jump reversal process has been observed for the elements with edges parallel to the $\langle 110 \rangle$ directions. The micromagnetic behavior of these epitaxial elements is substantially different from those of either continuous epitaxial Fe(001) films [E. Gu *et al.*, Phys. Rev. B **51**, 3596 (1995), C. Daboo *et al.*, Phys. Rev. B **51**, 15 964 (1995)] or polycrystalline elements in which the magnetocrystalline anisotropy is negligibly small. As the relative contributions of the in-plane shape and magnetocrystalline anisotropies can be modified by varying the element size, shape and orientation, these mesoscopic epitaxial elements not only offer an ideal model to study the roles of anisotropies in determining the micromagnetic structures but also allow the magnetic spin configuration to be controlled which could be useful for device applications, e.g., spin-polarized injection contacts and magnetic memory elements. [G. A. Prinz, Physics Today **48**(4), 58 (1995)]. [S0163-1829(98)04610-4]

I. INTRODUCTION

The art of growing epitaxial magnetic thin films has engendered fascinating new topics in fundamental magnetism research and has also offered possibilities for a range of technical applications. Epitaxial magnetic films with controllable magnetic anisotropies provide the experimentalist with an opportunity to study the interplay between dipolar (shape) and magnetocrystalline or interface anisotropies. In the case of ultrathin Fe/Cu(001)[1] and Co/Au(111)[2,3] films for example, the perpendicular spin orientation favored by the interface anisotropy is overwhelmed by the dipolar energy as the film thickness is increased. The question of how the micromagnetic structure evolves with thickness is important in gaining an understanding of how this transition occurs, and the domain structure which forms in the vicinity of the reorientation transition has therefore received much attention recently.[1–5] However, so far, the related question of how in-plane dipolar fields compete with in-plane anisotropies in determining the magnetic domain structure in epitaxial films has not been addressed. For a continuous two-dimensional (2D) epitaxial film with in-plane anisotropy, a single-domain state is predicted as the demagnetizing constant approaches zero.[6,7] Such a single-domain state has been observed in ultrathin Fe/Ag(001) (Ref. 8) and Co/Cu(001) films[9] and in 35–450 Å thick epitaxial Fe/GaAs(001) films.[10–12] On the other hand, if a thin-film structure has a lateral size which is comparable to or even smaller than a domain-wall thickness, a single-domain state will be again preferred regardless of the large stray field energy since no domain wall can form. However, between these two extreme cases, whether domains exist in epitaxial thin films and how the domain structures evolve with film in-plane dimensions and orientation are not clear. It is expected that novel micromagnetic phenomena may be observed by changing the film's lateral dimensions and orientation, i.e., making artificial mesoscopic epitaxial structures (elements). In this case, the micromagnetic structure will be determined by the interplay between in-plane shape and magnetocrystalline anisotropies, and the former is expected to become important when the film's lateral dimensions are reduced. Furthermore, since the magnetic anisotropy properties in these artificial structures can be controllably modified, it is expected these mesoscopic epitaxial structures will offer a range of applications. Various device applications of ferromagnetic metal-semiconductor epitaxial systems, such as spin-polarized injection contacts, have been suggested recently.[13]

Although a number of experimental investigations have been carried out on the micromagnetic structure supported by regular thin polycrystalline Permalloy elements,[14–18] to our knowledge no micromagnetic studies have been reported for thin epitaxial elements. The micromagnetic studies of epitaxial elements are substantially different from the size-dependent magnetic domain investigations of polycrystalline elements in which the magnetocrystalline anisotropies are negligibly small. In the present work, the in-plane dimension and orientation dependence of the domain structures and microscopic reversal processes in 150-Å-thick epitaxial Fe(001) elements were studied by Lorentz transmission electron microscopy (TEM). By comparing the domain structures and microscopic reversal behavior of continuous epitaxial Fe films of the same thickness which were studied extensively in our recent work,[10,11] the present work shows that the size, edge, and orientation of epitaxial Fe elements play an important role in determining their domain structures and microscopic reversal processes. A transition from single domain to multidomain remanent states has been observed by reducing the film dimension to $\sim 10\ \mu$m. At this size range, the domain structures and microscopic reversal processes of the epitaxial Fe elements are significantly different from those of larger elements and continuous films. Due to the interplay between in-plane shape and magnetocrystalline anisotropies, these epitaxial Fe elements show novel and controllable micromagnetic behavior.

II. SPECIMEN PREPARATION AND OBSERVATION TECHNIQUES

Lorentz TEM specimens must be sufficiently thin so as to permit the transmission of electrons. Furthermore, for magnetic domain studies, it is desirable to form such an electron transparent window far from the sample edge so that the influence of stray fields arising from the edges is greatly reduced. In this work, we used a selective chemical etching technique developed recently to prepare suitable window specimens.[10]

Arsenic-capped GaAs(001) substrates with a $Ga_{0.7}Al_{0.3}As$ etch stop layer supporting an molecular-beam epitaxy grown GaAs(001) epilayer (membrane) were used for epitaxial Fe film growth. The As cap layer on the GaAs(001) epilayer surface was desorbed in UHV before the film growth by annealing at 550 °C so as to get a clean and ordered GaAs surface.[19] During Fe growth, the pressure was less than 5×10^{-10} mbar and the film thickness was monitored by a quartz microbalance calibrated by a Dektak profilometer. The substrate temperature of 150 °C and a deposition rate of 1 Åmin^{-1} were used for the Fe growth. The epitaxial growth of bcc Fe was confirmed by *in situ* low-energy electron-diffraction and *ex situ* transmission electron diffraction. Finally, the completed Fe film was covered by a 15 Å Cr cap layer which can effectively prevent oxidation of the Fe film, as confirmed by electron energy-loss spectroscopy measurements.[20] Prior to element fabrication, the magnetic anisotropy properties of the continuous Fe film were characterized by magneto-optical Kerr effect (MOKE) vector magnetometry. MOKE measurements show the film has a predominant in-plane fourfold anisotropy with its easy axes parallel to the in-plane ⟨100⟩ directions as expected for an epitaxial bcc Fe film. Furthermore, from MOKE measurements, a weak uniaxial anisotropy ($K_u/K_1 \cong 0.1$) with its easy axis parallel to one of the hard axes ([110] direction) of the fourfold anisotropy has also been observed. Recent studies showed that this uniaxial anisotropy exists in other epitaxial Fe/GaAs(001) films[21] and the origin of this uniaxial anisotropy has been attributed to the surface atomic structure of the GaAs(001) surface.[22,23]

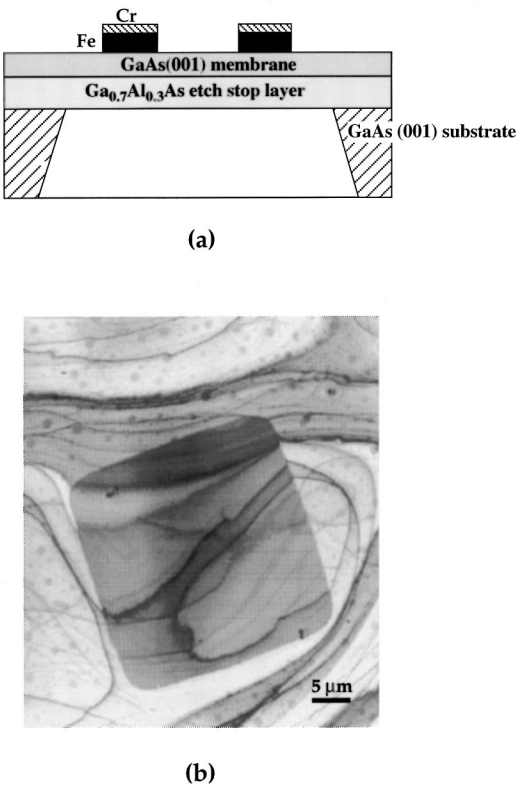

FIG. 1. (a) Cross-section schematic diagram of a Lorentz TEM specimen of epitaxial Fe elements prepared by optical lithography and selective chemical etching techniques, (b) Plane view TEM image of an epitaxial Fe(001) element supported on a GaAs single-crystal membrane.

Epitaxial square Fe elements with different size were fabricated utilizing optical lithography, ion milling and reactive etching techniques. The edges of these elements are parallel to either ⟨100⟩ easy or ⟨110⟩ hard directions. The thin GaAs(001) membrane which supports these epitaxial elements and is suitable for Lorentz TEM observation was formed by selective chemical wet etching from the back surface of GaAs(001) substrates. After fabrication, the structure and chemical composition of the elements were characterized by scanning electron microscopy (SEM), TEM, and energy-dispersive x-ray analysis (EDX). A cross-section schematic diagram of a completed Lorentz TEM specimen is shown in Fig. 1(a). Figure 1(b) shows a plane view TEM image of a $30 \times 30\ \mu\text{m}^2$ epitaxial Fe element. The dark bands shown in this image are bend contours arising from the single-crystal GaAs membrane. It can be seen that the edges of the element are relatively straight and smooth. EDX measurements confirmed that the Fe in the gaps between elements has been completely removed and that the thin Fe elements are well protected by the Cr cap layer.

Lorentz TEM is a desirable technique for the study of micromagnetic structures in micron or submicron size mag-

netic elements.[24,25] However, due to the difficulties of preparing Lorentz TEM specimens of epitaxial elements, this high-resolution technique has not been previously used to characterize their micromagnetic properties. In this work, using the specimen preparation technique described above, the magnetic domain structure and microscopic reversal processes in the epitaxial Fe elements were studied by using both a modified Philips CM20 and a JEOL 2000 FX Lorentz electron microscope. In both microscopes the specimen can be rotated in-plane by a driver and its orientation is determined by the electron-diffraction pattern. A magnetic field in the microscope thus can be applied in any in-plane direction with respect to the specimen to carry out *in situ* magnetizing experiments.

III. RESULTS AND DISCUSSION

A. Remanent domain structure

The studies of the remanent domain structures in these epitaxial Fe elements have been recently published elsewhere.[26] Here the main results are briefly summarized and further analyses are given, which will be helpful in order to analyze and explain the microscopic reversal processes of these epitaxial elements shown in the following sections.

The most important finding from these remanent domain structures is that thin epitaxial films with in-plane anisotropy transform into a multidomain state at remanence upon reducing their in-plane size and that for the 150-Å-thick film this transition occurs at a size of a few tens of microns. These results indicate that with decreasing element size, the in-plane demagnetizing field, which has been considered to be negligibly small for a thin epitaxial film,[7] becomes important in determining the domain structures. The demagnetizing field arises from the magnetic charges formed at element edges or domain walls. In the case that the elements with edges parallel to the ⟨100⟩ directions were initially magnetized along one of the ⟨100⟩ easy directions, the magnetization vector tends to remain in that direction upon reducing the applied field due to the magnetocrystalline anisotropy. Hence, magnetic charges would be uniformly distributed on the edges perpendicular to the magnetization vector. The demagnetizing fields arising from such uniformly distributed magnetic charges in square Fe elements with thickness 150 Å and different sizes were calculated and are shown in the Fig. 2. Our previous work showed that the coercive field, determined by the nucleation and unpinning of 90° domain walls of a continuous epitaxial Fe film of the same thickness, is about 8 Oe.[10] From Fig. 2 it can be seen that if an element has a size smaller than about $20\times 20\ \mu m^2$, the demagnetizing field within almost whole element becomes larger than the value of this nucleation field and for all the elements the demagnetizing field at the element edge is much larger than this nucleation field. Furthermore, there are always some imperfections at the element edges which may serve as nucleation centers. Thus, upon reducing the applied field, domain nucleation occurs at the element edges. Our studies show that for smaller elements these edge domains will develop to form a multidomain remanent structure and the configuration of the remanent domain structures in these epitaxial thin Fe elements is determined by the competition between dipolar interactions and magnetocrystalline anisotropy.[26]

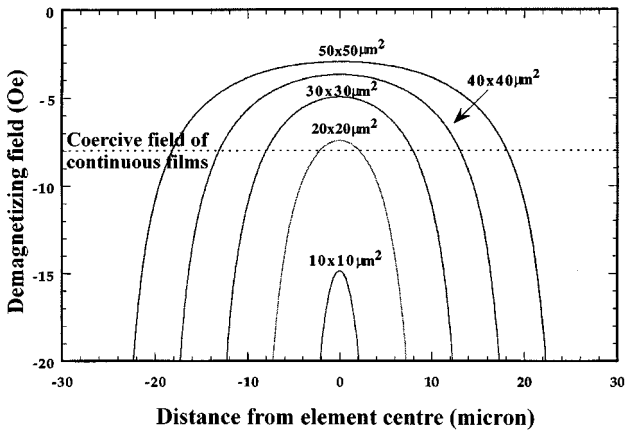

FIG. 2. Demagnetizing field distributions within 150 Å epitaxial elements of different size. Element edges are parallel to the ⟨100⟩ directions and the elements are assumed to be magnetized uniformly along one of in-plane ⟨100⟩ easy directions.

B. Microscopic reversal processes along the ⟨100⟩ easy directions

To carry out reproducible micromagnetic studies, it is important that the initial magnetic state is well defined. For reversal along the ⟨100⟩ easy directions, a ''single-domain'' state of elements was induced first by applying an initial magnetic field H_i ($H_i = 120$ Oe) parallel to one of the ⟨100⟩ easy axes. After removing the field, the microscopic reversal processes were studied by applying a reverse field H_r and simultaneously monitoring and recording the domain structure in the electron microscope. Figure 3 shows a series of Fresnel domain images of a $55\times 55\ \mu m^2$ element taken during reversal along the $[\bar{1}00]$ easy direction. The corresponding magnetization distributions in these images are shown in Fig. 4. It should be noted that most dark lines and bands shown in the images are bend contours coming from the single-crystal GaAs substrate. Minor tilting of the specimen allows these features to be distinguished unambiguously from the magnetic contrast of interest. Some defects have also been observed. These defects were induced during the process of fabricating elements. During reversal processes, the detailed local domain structures in the element may be perturbed by these defects as they act as pinning points.

As before, at remanence the element is almost in a single-domain state with small spike domains at the element edges. With respect to the reversal field, these edge domains have lower Zeeman energy. Therefore, upon increasing the reversal field, these edge domains expand quickly through 90° domain-wall displacements as shown in Figs. 4(a)–4(e). It is noticed that during the above processes, a new edge domain in which the magnetization is oriented parallel to the reversal field direction is nucleated. Upon increasing the reversal field, this reversed domain grew again through domain-wall displacements until the whole element was reversed [see Figs. 4(d)–4(h)]. The above reversal processes are similar to those observed in continuous epitaxial Fe films.[10,11] How-

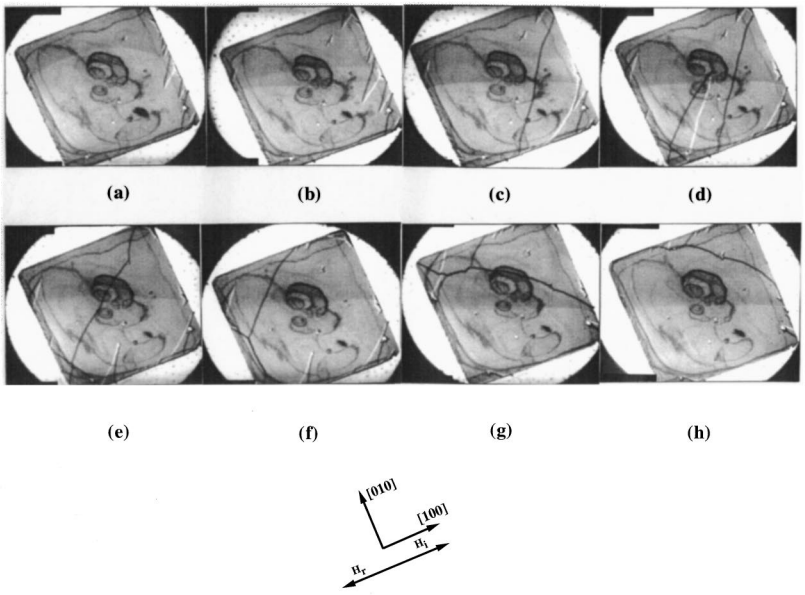

FIG. 3. Magnetic domain images of a 55×55 μm^2 Fe element with edges parallel to the $\langle 100\rangle$ directions during reversal along the [100] easy axis.

ever, some important differences due to the element edges were observed. Firstly the process of domain nucleation is influenced by the element edges, e.g., in order to reduce the magnetostatic energy, new domains nucleate only at those element edges where the magnetization is not originally parallel to the edges. Secondly, an irregular flux closure checkerboard domain pattern was observed during the reversal processes. This checkerboard domain pattern is constructed by domains in which the magnetizations are oriented along the four easy directions of the fourfold anisotropy, respectively. For continuous epitaxial Fe films, our earlier work showed that the checkerboard domain structures were only observed for epitaxial films with a predominant fourfold anisotropy, i.e., the ratio of uniaxial to the fourfold anisotropies K_u/K_1 should be smaller than 1%. Therefore the checkerboard domain formation in the continuous Fe films is mainly due to the in-plane fourfold symmetry in the magnetocrystalline energy. The ratio K_u/K_1 of the continuous epitaxial Fe film from which the elements were fabricated was determined to be about 10%. This uniaxial anisotropy makes the real easy axes depart slightly from the crystalline cubic $\langle 100\rangle$ directions [as shown by the dashed lines in Fig. 4(a)] and therefore causes the magnetization to jump during reversal from the initial $[1\bar{0}0]$ direction to the $[0\bar{1}0]$ direction rather than to both the $[0\bar{1}0]$ and [010] directions to form a checkerboard domain structure. The formation of the local flux closure checkerboard domain pattern in the element is caused by edge effects. In order to reduce the magnetostatic energy, the magnetization within the edge domains tends to orient parallel to the element edges. As the element edges are

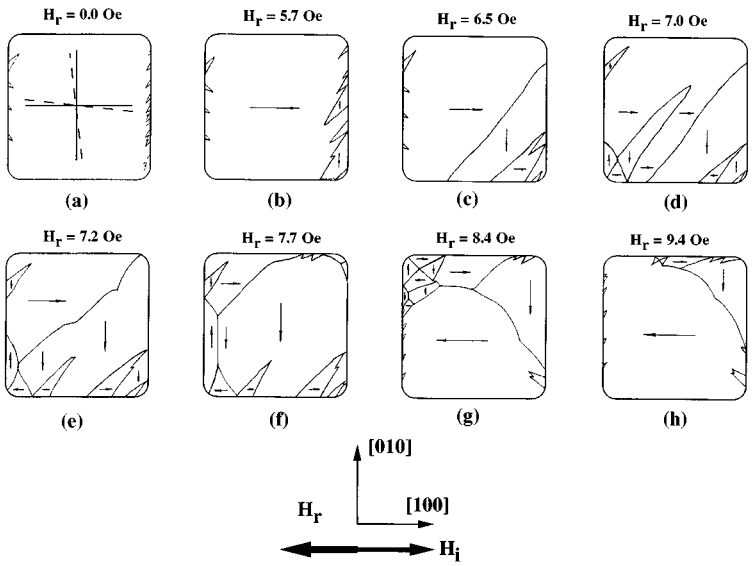

FIG. 4. The magnetization schematics of the domain images shown in Fig. 3.

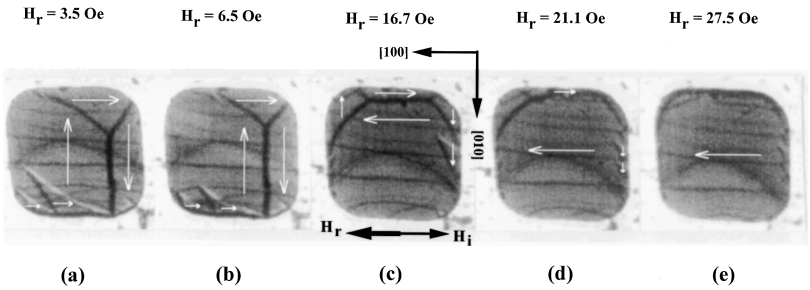

FIG. 5. Magnetic domain structures of a $12\times12\ \mu m^2$ epitaxial Fe element with edges parallel to the ⟨100⟩ directions during reversal along the [100] easy axis.

parallel to the ⟨100⟩ easy directions, the configuration with the magnetization parallel to the edges also decreases the magnetocrystalline anisotropy energy. On the other hand, the magnetization orientation adopted should also minimize the formation of magnetic charges at domain walls by keeping the perpendicular components of magnetization approximately continuous across the domain walls. To satisfy these conditions, when the edge domains expand and come into contact with each other, the checkerboard domain pattern develops in the Fe element. Thus, although the checkerboard domain patterns were observed for both continuous epitaxial Fe films and Fe elements, their origins differ.

Since the remanent domain structures of the $55\times55\ \mu m^2$ and $12\times12\ \mu m^2$ elements are significantly different,[26] it is expected that they will show different reversal behavior. Figure 5 shows the domain structures and magnetization distributions of a $12\times12\ \mu m^2$ element with edges parallel to the ⟨100⟩ directions during reversal along the [100] direction. On the application of a reverse field, the domains in which the magnetization was antiparallel to the reverse field shrank. This continued until a critical field, denoted H_{c1} ($H_{c1}=16.4$ Oe), was attained whereupon the unfavorably oriented domains disappeared and an irreversible change took place [between Figs. 5(b) and 5(c)]. At this transition field, a domain with the magnetization oriented along the reverse field direction nucleated at the bottom edge and expanded rapidly. As this favorably oriented domain grew, the original vertical 180° domain wall parallel to the [010] direction in Fig. 5(b) became shorter and finally disappeared and immediately a 180° domain wall parallel to the [100] direction appeared as shown in Fig. 5(c). Although the actual transition was too rapid to record, the key to this transition was that the orientation of the 180° wall changed by 90° to facilitate an increase in size of the favorably oriented domain. A further increase in the reverse field caused the movement of the 180° domain wall towards the element edge and only by applying a strong reverse field ($H_r=35$ Oe) could the 180° wall be driven into the side of the element. Furthermore, it was found that after the 180° domain wall was driven into the side of the element, on reduction of the field, the domain structure with the 180° wall parallel to the [100] direction could regenerate. Decreasing the field further to H_{c2} which satisfies $0<H_{c2}<H_{c1}$ resulted in a transition back to a domain structure similar to that shown in Fig. 5(a). Not much change in the domain configuration was observed when further decreasing the field from H_{c2} to zero.

From the above images and analyses, it can be seen that for reversal along the ⟨100⟩ easy direction the $55\times55\ \mu m^2$ and $12\times12\ \mu m^2$ elements with edges parallel to the ⟨100⟩ directions show very different remanent domain structures and reversal behavior. For the $55\times55\ \mu m^2$ large element, the reversal takes place via a combination of two 90° magnetization reorientations. This process is similar to that observed in continuous epitaxial Fe films[10] although the detailed domain configuration is perturbed by the element edges. For the $12\times12\ \mu m^2$ element, the reversal proceeds mainly via 180° domain-wall reorientation and displacements.

By applying the field along the ⟨100⟩ directions, the microscopic reversal processes of the epitaxial elements with edges parallel to the ⟨110⟩ directions have also been studied. The domain images and corresponding magnetization distributions of such a $12\times12\ \mu m^2$ element during reversal is shown in Fig. 6. At remanence the element supports a stripe multidomain structure with magnetization oriented parallel to either the [100] or $[0\bar{1}0]$ easy directions. Increasing the reversal field results in the [100] oriented domains (which have a lower Zeeman energy) growing through 90° domain-wall displacements. Further increasing the applied field forces domain walls into contact in the middle of element as shown in Fig. 6(c). In this image, almost the whole element was oriented along the [100] direction and only the two element corners remained oriented parallel to the $[0\bar{1}0]$ direction in order to minimize the magnetostatic energy. Again a strong field ($H_r=32$ Oe) is needed to drive these corner do-

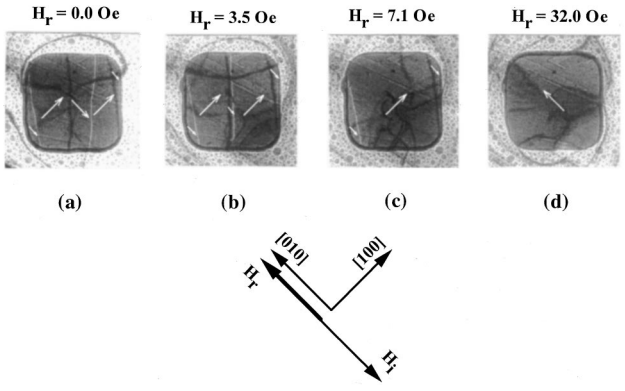

FIG. 6. Magnetic domain structures of a $12\times12\ \mu m^2$ Fe element with edges parallel to the ⟨110⟩ directions during reversal along the [010] easy axis.

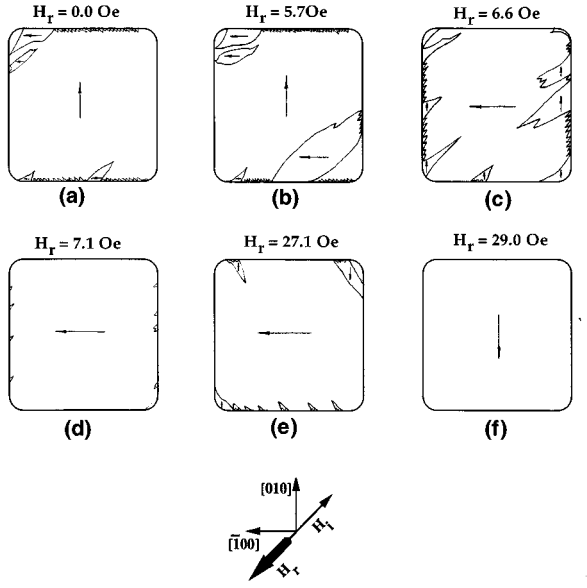

FIG. 7. Magnetization schematics of a $55\times55\ \mu m^2$ Fe element with edges parallel to the ⟨100⟩ directions during reversal near the [110] hard axis.

main walls into the element edge to realize a [100]-oriented single-domain state. After the element was driven into the single-domain state, further increase of the reversal field did not cause the element to split into a multidomain structure again. However, it is found that at a high critical reversal field, one dark band along an element edge jumped suddenly to the opposite edge [compare Fig. 6(c) with Fig. 6(d)]. These dark bands arise from the electron deflection occurring at the element edges due to the Lorentz force. The deflection direction is determined by the orientation of the magnetization vector at the edge. If the electrons are deflected at an edge towards the element, a dark band appears at this edge. Thus, from Fig. 6(c) and Fig. 6(d) which show that the dark band jumps to the opposite edge, we can deduce that further reversal at the high reversal field took place by the magnetization coherently jumping 90° from being parallel to the [100] to the [010] direction. Such a 90° coherent jumping reversal process has never been observed for continuous epitaxial Fe films. Clearly, the reversal process shown in Fig. 6 is remarkably different from that of the element with the same size but with edges parallel to the ⟨100⟩ directions.

C. Microscopic reversal processes along the ⟨110⟩ hard directions

To investigate the magnetization reversal processes along the ⟨110⟩ hard directions, the epitaxial Fe elements were rotated through 45° in the microscope so that one of the ⟨110⟩ directions, say the [110] direction, lay parallel to the field direction. Following a similar procedure to that used for the ⟨100⟩ directions, a single-domain state was induced by applying an initial field H_i along [110]. Magnetization reversal was then studied by applying successively greater fields parallel to [110].

Figure 7 shows the domain structures and magnetization distributions of a $55\times55\ \mu m^2$ element during reversal. The edges of this element are parallel to the ⟨100⟩ easy directions.

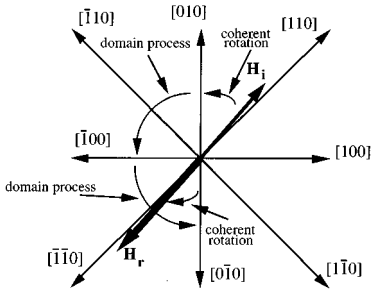

FIG. 8. Magnetization reversal process of continuous epitaxial Fe films for applied fields near the [110] hard direction.

From these patterns, the overall magnetization reversal process can now be explained with reference to Fig. 8. While [110] lies midway between the easy [100] and [010] directions, in practice, the applied field will not be exactly along the intended direction. Thus, as the field strength is reduced from a high value along a direction close to the [110] axis, the magnetization will coherently rotate towards the nearest easy axis ([010] in Figs. 7 and 8). It is found that after removal of the initial field small spike domains formed at the edges parallel to the [100] direction [see Fig. 7(a)]. This domain structure shows that at remanence the element is almost in a single-domain state with magnetization vector parallel to the [010] direction and only in the small edge domains the magnetization is parallel to the element edges. Application of a field of the opposite polarity (i.e., parallel to $[1\bar{1}0]$) causes the edge domains in which the magnetization is oriented along [100], the easy direction near to that of the applied field, to grow. Increasing the field strength by only a fraction of 1 Oe allows $[\bar{1}00]$-oriented domains to grow through Barkhausen-like jumps which were observed directly on the microscope screen. The observed domain-wall jumps are due to wall unpinning. The jump direction is along $[\bar{1}10]$, that is, perpendicular to the field direction. When it is complete the whole of the film is once again almost uniformly magnetized but the direction of magnetization has changed from being along [010] to lying along [100]. Increasing the reverse field strength to the second critical value leads to the nucleation and expansion of new domains in which the magnetization is now oriented close to the $[0\bar{1}0]$ direction. It is important to note that the domain walls at this stage are oriented almost along the $[\bar{1}10]$ direction rather than the [110] direction as was the case in the first domain process. These new domains grow quickly again through Barkhausen-like jumps until the element reaches the third single-domain state [Fig. 7(f)] in which the magnetization is oriented close to the [010] direction. Increasing the field strength further leads to a coherent rotation of the magnetization away from the [010] direction towards that of the applied field until the element is saturated. The description given above is in accord with the magnetization distributions shown in Figs. 7(a)–7(f). If the applied field was initially closer to [100] rather than to [010] similar processes would be involved although the magnetization vector would now change in a clockwise sense during reversal. Coherent rotation would be responsible for the initial and final stages as before. In general, the above reversal processes are similar to the reversal behavior observed in continuous epitaxial thin

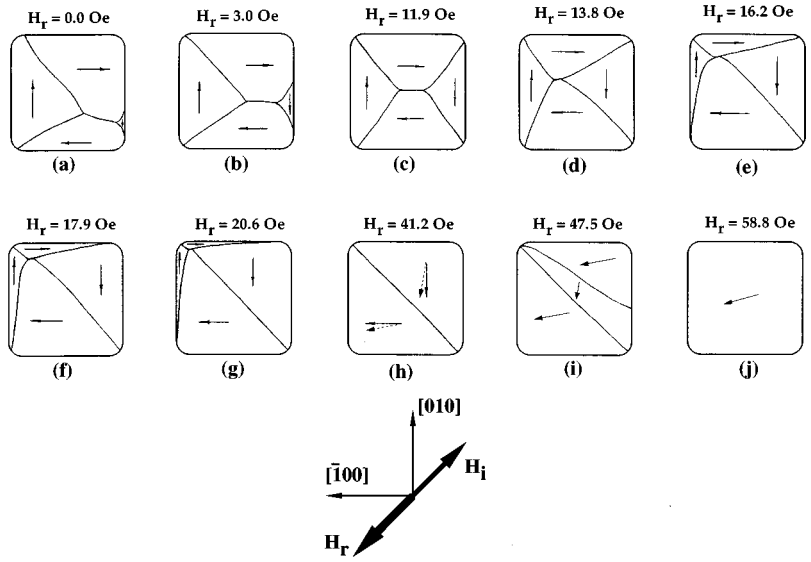

FIG. 9. Magnetization schematics of a 12×12 μm^2 Fe element with edges parallel to the $\langle 100\rangle$ directions during reversal near the [110] hard axis.

Fe films.[10,11] However, the detailed domain configuration is perturbed by the element edges. For example, when domains expand to touch the element edges, spike domain walls appear in order to avoid the formation of magnetic charges at the edges.

For a field applied along the hard axis, again, strikingly different magnetization reversal behavior was observed for the 12×12 μm^2 epitaxial elements. Figures 9(a)–9(j) show schematically the domain structures and magnetization distributions of a 12×12 μm^2 element with edges parallel to the $\langle 100\rangle$ directions during reversal along the [110] hard axis. In the remanent state [Fig. 9(a)], this element shows a flux closure multidomain structure. On the application of a reversal field, the favorably oriented two domains in which magnetizations were parallel to the $[010]$ and $[\bar{1}00]$ directions, respectively, grew at the expense of those less favorably oriented through domain-wall displacements. An increase in the reversal field caused further movement of the domain walls and the domain pattern became very distorted. It can be seen that as the domain walls were driven close to the element edges, they became more bowed and parallel to the edges as shown in Fig. 9(f). At the same time, the length of the 180° domain wall became shorter and finally disappeared. When the reversal field is higher than 34 Oe, only one domain wall remained and the rest had been driven into the element edges as shown in Fig. 9(h). At this stage, it can be seen that the remaining domain wall became an almost straight line oriented along the diagonal direction of the element. This domain configuration was maintained in a large reversal field range until the reversal field was increased to $\sim$50 Oe. The reason why this domain structure is stable is because the angles between the magnetization vectors in the two domains and the reversal field are almost the same. It should be noted that at the high reversal fields, the magnetization vectors which were originally aligned along the $\langle 100\rangle$ easy axes would rotate from the easy axes towards the field direction as shown by the dashed arrows in Fig. 9(h). Since in practice the field cannot be exactly aligned along the bisector direction (hard axis), one domain orientation was always more favorable than the another. Therefore, at very high reverse field, the favorable domains would nucleate and grow from the element edge as shown in Fig. 9(i) and when it finished, the element reached a single-domain structure with its magnetization oriented near the $[\bar{1}00]$ direction which is the easy axis closest to the field direction. Increasing the field further would result in the magnetization rotating coherently to the field direction.

For reversal along the $\langle 110\rangle$ hard direction, the 12×12 μm^2 epitaxial elements with edges parallel to the $\langle 110\rangle$ directions show distinct and relatively simple reversal behavior. In this case, a magnetic field was again first applied along the [110] direction to induce the initial single-domain state. At remanence, the element supported a stripe multidomain structure as shown in Fig. 10(a). As discussed in Ref. 26, such a stripe domain structure can reduce greatly the magnetostatic energy. Upon reversing the field and increasing the reverse field strength, the $[\bar{1}00]$-oriented domains which have lower Zeeman energy grew and became predominant as shown in Fig. 10(b). In this domain structure,

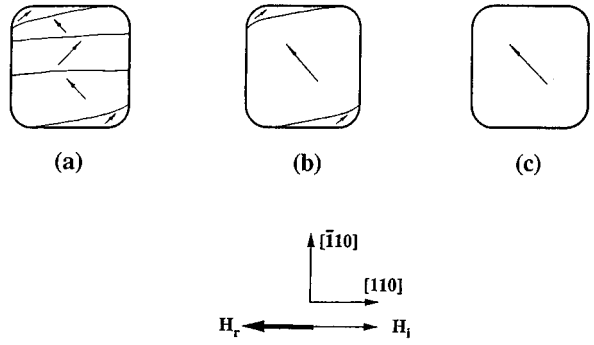

FIG. 10. Magnetization schematics of a 12×12 μm^2 Fe element with edges parallel to the $\langle 110\rangle$ directions during reversal along the [110] hard axis.

small domains with magnetization oriented along the [010] directions remained only at the two corners in order to minimize the magnetostatic energy. These small corner domains shrank upon further increasing the reverse field. After the element reached a [100]-oriented single-domain state, further increasing the reversal field caused the magnetization to rotate coherently towards the field direction.

During the above reversal processes, we deliberately reduced the magnetic field in several stages. Lorentz microscopy measurements revealed that the domain structures shown in Figs. 9 and 10 were reversible. It is found that upon decreasing the field from the value sufficient to drive all the domain walls into the element edge, the whole domain patterns shown in Fig. 9 can still be regenerated. This behavior is different from the reported reversal behavior occurring in the polycrystalline permalloy elements where once the domain walls were driven into contact with the edges of the elements, very complex domain structures would appear as the applied field was reduced.[15] It has been pointed out that these complex domain structures were caused by the imperfections at the element edges. The fact that the same domain patterns can be regenerated in these epitaxial Fe elements suggests that the edges of these elements are smooth and have less defects. The other possible reasons for regenerating the same domain structures in these epitaxial Fe elements may be that they have (a) a strong magnetocrystalline anisotropy which favors a well-defined domain structure and (b) a large magnetic moment which increases the energy penalty for disordered domain structures.

Furthermore, the above measurements show that for a field applied along the hard axis, a small misalignment between the applied field and hard axis will make the magnetization first rotate coherently towards the nearest easy axis upon reducing the initial field. However, it is found that if the applied field and the hard axis are carefully aligned, reducing the field resulted in a fine-scale stripe domain structure developing first as shown in Fig. 11. The fine stripes in the images correspond to the areas of clockwise (towards the [100] easy direction) and anticlockwise (towards the [010] easy direction) rotated magnetization vectors apart from the hard axis. Initially, the width of stripes was only a few hundred nanometers and the magnetic contrast was lower. Upon decreasing the field, the width of the stripes broadens and magnetic contrast increases as shown in Fig. 11(c). The corresponding magnetization schematic of this image is shown in Fig. 11(d). For continuous epitaxial Fe films, such fine-scale stripe domain structures have also been observed but they occur only when the angle between the ⟨110⟩ hard axis and applied field is smaller than 0.1°.[27] Outside this angular range, upon decreasing the field, the magnetization vector rotates coherently towards the nearest easy axis. For the continuous epitaxial Fe films, the fine-scale stripe domain structures were attributed to be a consequence of a domain splitting process arising from local film structural inhomogeneity.[27] Our experiments showed that for the 12 $\times 12\ \mu m^2$ epitaxial elements such fine-scale stripe domain structures can occur for the field applied within about 1° of the hard axis. The reason why for small epitaxial elements the initial fine-scale stripe domain structure could be observed within a larger angular range is again due to the role of the in-plane demagnetizing field. If initially the magnetization vector coherently rotates towards one easy axis, say [100] due to a small misalignment between applied field and the hard axis, the demagnetizing field which is oriented along the direction opposite to the magnetization vector will rotate towards the [100] direction. The resultant field of this demagnetizing field and the applied field will make the magnetization rotate towards the [010] direction in the areas where the local hard axes deviate slightly from the [110] towards the [100] direction due to the local structural inhomogeneity. Thus, the initial fine-scale stripe domain structure can still be formed. For the continuous epitaxial films, as the demagnetizing field is negligibly small, the fine stripe domain structure only occurs when the applied field and the hard axis are well aligned.

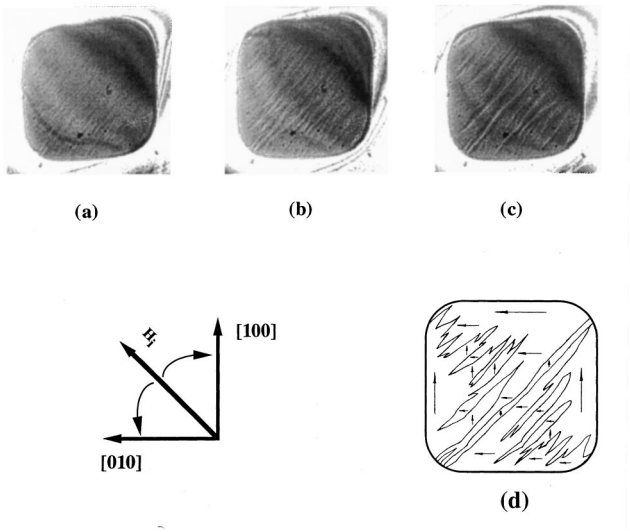

FIG. 11. The fine-scale stripe domain structures of a 12 $\times 12\ \mu m^2$ epitaxial Fe element with edges parallel to the ⟨100⟩ directions. These domain structures develop upon decreasing the initial applied field H_i [H_i in image (a) $> H_i$ in (b) $> H_i$ in (c)] which is well aligned along the [110] hard axis.

These measurements show that due to the in-plane magnetocrystalline anisotropy, the reversal processes of the epitaxial elements along the ⟨110⟩ hard axes are significantly different from the reversal behavior along the ⟨100⟩ easy axes. Again, striking differences in the microscopic reversal processes were observed for the elements with different size. For the small elements with the same $12 \times 12\ \mu m^2$ size, the element orientation plays an important role in determining their reversal behavior.

IV. SUMMARY

In summary, we have investigated the in-plane size and orientation dependence of micromagnetic structures and microscopic reversal processes in epitaxial Fe elements by Lorentz electron microscopy. Upon reducing the element lateral dimensions, a transition from a single-domain to a multidomain remanent state has been observed. For 150-Å-thick epitaxial Fe elements such dramatic changes in the remanent domain structure and microscopic reversal behavior occur when the element size is reduced to $\sim 10\ \mu m$. The transition can be explained as a consequence of the in-plane dipolar contribution to the total energy becoming comparable to that

of the magnetocrystalline anisotropy at this size. Due to the interplay between in-plane shape and magnetocrystalline anisotropies, distinct micromagnetic structures arise according to not only the crystallographic direction along which the field is applied but also the orientation of the element edges. These results illustrate that novel micromagnetic behavior can be controllably induced in these model ''mesoscopic'' structures and these mesoscopic epitaxial elements provide a new approach to the study of competing in-plane shape and magnetocrystalline anisotropies.

This work also shows that magnetizing experiments carried out in an electron microscope can provide a wealth of information on the microscopic magnetization process within small epitaxial elements. Such information is extremely useful for understanding the macroscopic magnetic behavior of these epitaxial elements and is relevant to practical device applications.

ACKNOWLEDGMENTS

The financial support of the EPSRC and the Newton Trust, Cambridge for this work is greatly acknowledged. We also thank Professor H. Ahmed, Dr. S. J. Gray, Dr. C. Daboo, and Dr. D. A. Ritchie for their help with the work.

[1] R. Allenspach and A. Bischof, Phys. Rev. Lett. **69**, 3385 (1992).
[2] R. Allenspach, M. Stampanoni, and A. Bischof, Phys. Rev. Lett. **65**, 3344 (1990).
[3] M. Speckmann, H. P. Oepen, and H. Ibach, Phys. Rev. Lett. **75**, 2035 (1995).
[4] G. Bochi, H. J. Hug, D. I. Paul, B. Stiefel, A. Moser, I. Parashikov, H. J. Guntherodt, and R. C. O'Handley, Phys. Rev. Lett. **75**, 1839 (1995).
[5] G. Bochi, C. A. Ballentine, H. E. Inglefield, C. V. Thompson, R. C. O'Handley, H. J. Hug, B. Stiefel, A. Moser, and H. J. Güntherodt, Phys. Rev. B **52**, 7311 (1995).
[6] C. Kittel, Phys. Rev. **70**, 965 (1946).
[7] R. Allenspach, J. Magn. Magn. Mater. **129**, 160 (1994).
[8] J. L. Robins, R. J. Celotta, J. Unguris, D. T. Pierce, B. T. Jonker, and G. A. Prinz, Appl. Phys. Lett. **52**, 1918 (1988).
[9] H. P. Oepen, J. Magn. Magn. Mater. **93**, 116 (1991).
[10] E. Gu, J. A. C. Bland, C. Daboo, M. Gester, L. M. Brown, R. Ploessl, and J. N. Chapman, Phys. Rev. B **51**, 3596 (1995).
[11] C. Daboo, R. J. Hicken, E. Gu, M. Gester, S. Gray, E. Ahmad, J. A. C. Bland, R. Ploessl, and J. N. Chapman, Phys. Rev. B **51**, 15 964 (1995).
[12] E. Gu, C. Daboo, J. A. C. Bland, M. Gester, A. J. R. Ives, L. M. Brown, N. A. Stelmashenko, and J. N. Chapman, J. Magn. Magn. Mater. **126**, 180 (1993).
[13] G. A. Prinz, Phys. Today **48** (4), 58 (1995).
[14] D. A. Herman, Jr., B. E. Argyle, and B. Petek, J. Appl. Phys. **61**, 4200 (1987).
[15] B. W. Corb, J. Appl. Phys. **63**, 2941 (1988).
[16] E. J. Ozimek, J. Appl. Phys. **57**, 5406 (1985).
[17] S. McVitie and J. N. Chapman, IEEE Trans. Magn. **24**, 1778 (1988).
[18] S. J. Hefferman, J. N. Chapman, and S. McVitie, J. Magn. Magn. Mater. **95**, 76 (1991).
[19] U. Resch, N. Esser, Y. S. Raptis, W. Richter, J. Wasserfall, A. Forster, and D. I. Weatwood, Surf. Sci. **269**, 797 (1992).
[20] J. Yuan, E. Gu, M. Gester, J. A. C. Bland, and L. M. Brown, J. Appl. Phys. **75**, 6501 (1994).
[21] R. J. Hicken, D. E. P. Eley, M. Gester, S. J. Gray, C. Daboo, A. J. R. Ives, and J. A. C. Bland, J. Magn. Magn. Mater. **145**, 278 (1995).
[22] J. J. Krebs, B. T. Jonker, and G. A. Prinz, J. Appl. Phys. **61**, 2596 (1987).
[23] M. Gester, C. Daboo, R. J. Hicken, S. J. Gray, A. Ercole, and J. A. C. Bland, J. Appl. Phys. **80**, 347 (1996).
[24] J. N. Chapman, J. Phys. D **17**, 623 (1984).
[25] J. N. Chapman, S. McVitie, and S. J. Hefferman, J. Appl. Phys. **69**, 6078 (1991).
[26] E. Gu, E. Ahmad, S. J. Gray, C. Daboo, J. A. C. Bland, L. M. Brown, M. Rührig, A. J. McGibbon, and J. N. Chapman, Phys. Rev. Lett. **78**, 1158 (1997).
[27] U. Ebels, M. Gester, C. Daboo, and J. A. C. Bland, Thin Solid Films **275**, 172 (1996).